

Articles

Effects of Deglycosylation of Sodium Channels on Their Structure and Function[†]

Nora B. Cronin,[‡] Andrias O'Reilly,[‡] Hervé Duclouhier,^{§,||} and B. A. Wallace^{*,‡,⊥}

Department of Crystallography, Birkbeck College, University of London, London WC1E 7HX, U.K., BBSRC Centre for Protein and Membrane Structure and Dynamics, CCLRC Daresbury Laboratory, Warrington WA4 4AD, U.K., and UMR 6026 CNRS-Université de Rennes I, Laboratoire des Interactions Cellulaires et Moléculaires, Campus de Beaulieu, Bâtiment 13, 35042 Rennes Cedex, France

Received June 17, 2004; Revised Manuscript Received October 15, 2004

ABSTRACT: Voltage-gated sodium channels are important membrane proteins underlying electrical signaling in the nervous and muscular systems. They undergo rapid conformational changes between closed resting, activated, and inactivated states. Approximately 30% of the mass of the sodium channel is carbohydrate, present as glycoconjugate chains, mostly composed of *N*-acetylhexosamines and sialic acid. In this study, the effects of removing the carbohydrate on the functional and structural properties of highly purified sodium channels from *Electrophorus electricus* were investigated. After enzymatic deglycosylation, channels were reconstituted into planar lipid bilayers. In the presence of batrachotoxin, substates became evident and the single-channel conductance of the deglycosylated channels was slightly reduced relative to that of native channels, consistent with electrostatic effects due to the reduction in negative charge at the extracellular vestibule of the channel. The previously reported state-dependent changes in the circular dichroism spectra that are associated with the binding of the anticonvulsant drug Lamotrigine and batrachotoxin are also seen in the modified channels. Synchrotron radiation circular dichroism (SRCD) spectroscopy on the type of sugars found in the sodium channel showed that unlike most carbohydrates, these sugars produce a significant dichroic signal in the far-ultraviolet region. This can account for all of the measured SRCD-detected spectral differences between the native and deglycosylated channels, thereby indicating that no net change in protein secondary structure results from the deglycosylation procedure. Furthermore, thermal denaturation studies detected no significant differences in stability between native and deglycosylated channels. In summary, while the sugars of the voltage-gated sodium channels from electroplax are not essential for functional or structural integrity, they do appear to have a modulating effect on the conductance properties of these channels.

Voltage-gated sodium channels underlie action potential initiation and propagation in nerves and muscles and are also

involved in various pathophysiological and channelopathies due to inherited mutations (1). Their functions, whether *in situ* or after heterologous expression and reconstitution into

[†] This work was funded by Project Grant B15499 from the BBSRC (to B.A.W.), a seed grant from the CNRS and the Royal Society (to H.D. and B.A.W.), an international cooperation grant from the Wellcome Trust (to B.A.W. and H.D.), and an equipment grant from the CNRS (to H.D.). The circular dichroism instrumentation was supported, in part, by Grant B14225 from the BBSRC (to B.A.W.). The SRCD beam time was provided by a grant from the CCLRC (to B.A.W.). A.O'R. was supported by the H. W. Fletcher Studentship from the British Heart Foundation.

* To whom correspondence should be addressed. Phone: +44-207-631-6857. Fax: +44-207-631-6803. E-mail: ubcg25a@mail.cryst.bbk.ac.uk.

[‡] University of London.

[§] UMR 6026 CNRS-Université de Rennes I.

^{||} Present address: Institut de Physiologie et de Biologie Cellulaires, UMR 6187 CNRS-Université de Poitiers, 86022 Poitiers Cedex, France.

[⊥] CCLRC Daresbury Laboratory.

planar lipid bilayers, have been extensively characterized, but details of their structures and the molecular basis of their voltage-dependent gating remain largely unknown. Recently, the secondary structure of the voltage-gated sodium channel from the electric eel *Electrophorus electricus* was examined by circular dichroism (CD)¹ spectroscopy (2). The channel proteins were found to be largely helical, consistent with previous structural predictions based on the extensive transmembrane regions identified in their sequences (3), and their homology with known potassium channel structures (4, 5). Those CD studies also detected significant state-dependent conformational changes upon binding of the anticonvulsant drug Lamotrigine (LTG) and the neurotoxin batrachotoxin (BTX) to the channels (2).

Sodium channels exhibit strong sequence conservation across species and tissue-specific types (6, 7). The sodium channel from *E. electricus* has only a single α -subunit, unlike many other voltage-gated ion channels which can have a number of auxiliary regulatory subunits in addition to the channel-forming α -subunits (8, 9). From its cDNA sequence (3), the protein is predicted to consist of 1820 amino acids, with a corresponding molecular mass of 208 kDa. Its sequence contains four highly homologous internal repeats (designated domains I–IV), each of which is comprised of six transmembrane-spanning segments (S1–S6) and a pore loop, with linking regions between the domains, and extended aqueous soluble N- and C-terminal domains. Sugar moieties are covalently linked to the protein at several sites in the extracellular loops between S5 and S6 (10), and comprise ~30% of the total molecular mass of the channel, resulting in a heterogeneous mixture of glycoprotein molecules in the range of ~280–300 kDa (11). The carbohydrate is mainly composed of *N*-acetyl amino sugars, both uncharged in the case of *N*-acetylhexosamines (45%) and negatively charged in the case of *N*-acetylneuraminic acid (sialic acid) (40%); the remaining sugars are mostly mannose and galactose (12). A striking feature of the sialic acid is that it exists as extended chains of polysialic acid. This form is rare in vertebrates, being thus far found only in neurons, muscle cells, and human milk (13).

The sialic acids have been estimated to contribute ~110–130 negative charges (11) to the external surface of the channel; it has been postulated that this charge modulates the electric field experienced by the channel voltage-sensing mechanism (14). This role for the sialic acids is consistent with electrophysiological experiments: removal of sialic acid by either desialylation or expression of channels with mutations at the putative glycosylation sites resulted in shifts of the conductance–voltage curves of ~10 mV in a depolarizing direction (14). Whether the observed alteration in the conductance–voltage curve can be attributed simply to electrostatic changes, or to modified channels undergoing conformational changes resulting in altered voltage sensitivities, was unclear.

In this study, a number of functional and structural properties of native and fully deglycosylated sodium channels were compared to determine the underlying reason for the

observed functional changes. Single-channel conductance studies in planar bilayers in the presence of batrachotoxin (BTX), which results in steady-state activation, were undertaken to compare functional properties of native and deglycosylated channels. Drug-induced CD spectral changes associated with ligand binding were also examined to determine if similar effects were found as with the native channel, a further measure of functional integrity. To investigate the structural consequences of deglycosylation, synchrotron radiation circular dichroism (SRCD) spectroscopy was then used to examine the secondary structures of the channels with and without sugars, and to compare their difference spectra to spectra of isolated sugars. Finally, thermal denaturation studies were carried out to compare the conformational stabilities of the deglycosylated and native channels.

EXPERIMENTAL PROCEDURES

Materials

Genapol C-100 (10% solution) was obtained from Calbiochem. IgM anti- α -2,8-*N*-acetylneuraminic acid was purified as previously described (2) from horse antiserum, a gift from R. Schneerson of the National Institute of Child Health and Human Development (Bethesda, MD) (15). Lamotrigine was a gift from R. W. Janes of Queen Mary College of the University of London. Batrachotoxin was a gift from J. W. Daly of the National Institute of Diabetes and Digestive and Kidney Diseases (Bethesda, MD). Polyacrylydrazido-agarose, protease inhibitors, rabbit anti-horse IgG, colominic acid (poly-2,8-*N*-acetylneuraminic acid), wheat germ lectin immobilized on cross-linked 4% beaded agarose (WGA), and *N*-acetyl-D-glucosamine (NAG) were all purchased from Sigma Aldrich. CNBr-activated Sepharose 4B Fast Flow, ANX Sepharose 4 Fast Flow, and HiPrep Sephacryl S300 High Resolution 16/60 columns were from Amersham Pharmacia, and PVDF membranes were from BDH Laboratory Supplies. PNGase F was purchased from New England Biolabs. *N*-Acetylchitopentose (a pentamer of NAG) was purchased from AMS Biotechnology (Europe) Ltd. Float-A-Lyzer dialysis tubes (100K MW cutoff) were purchased from Perbio-Science UK, and Ultracel Amicon YM100 membranes were from Millipore.

The lipids used for planar lipid bilayer studies were egg phosphatidylcholine (PC) from Sigma Aldrich and palmitoylphosphatidylethanolamine (PE) and palmitoyl-oleoylphosphatidylserine (PS) from Avanti Polar Lipids.

Methods

Purification and Deglycosylation of Sodium Channels. Sodium channels were purified from *E. electricus* as previously described (2) using an anti- α -2,8-*N*-acetylneuraminic acid antibody column. Alternatively, the protein was purified in higher yield on a lectin affinity column. The solubilized membranes (60 mL) were bound to an ANX Sepharose 4 Fast Flow ion exchange column and washed initially with buffer A [50 mM sodium phosphate (pH 6.8), 0.1% Genapol C-100, 1 mM EGTA, and 5 mM EDTA], subsequently with a step gradient of buffer A containing 0.4 M KCl, and finally eluted with a step gradient of 0.8 M KCl in the same buffer. Fractions containing the sodium channel were identified on

¹ Abbreviations: BTX, batrachotoxin; CD, circular dichroism; LTG, Lamotrigine; NAG, *N*-acetylglucosamine; PC, phosphatidylcholine; PE, phosphatidylethanolamine; PS, phosphatidylserine; SRCD, synchrotron radiation circular dichroism; TTX, tetrodotoxin.

Daresbury, on station CD12. Samples of sodium channels (both native and deglycosylated) in 20 mM sodium phosphate (pH 7.4) and 0.05% Genapol at ~ 1 mg/mL protein (the final protein concentrations were determined according to quantitative amino acid analysis) were examined in a 0.005 cm Suprasil cell (Hellma UK, Ltd.). Three spectra and three baselines were collected at 1 nm intervals over a wavelength range from 300 to 165 nm. The spectra were averaged, baseline subtracted, and smoothed with a Savitsky–Golay filter. Sugar (colomonic acid or chitopentose) spectra were collected in a similar manner, except using a cell with a path length of 0.001 cm and a concentration of 20 mg/mL in distilled water; sugar baselines were distilled water.

Conductance Measurements in Planar Lipid Bilayers. Single-channel and macroscopic conductance measurements of the purified native and deglycosylated sodium channels were performed as previously described for native channels (2) using the tip-dip method (17); i.e., bilayers were formed at the tip of patch–clamp pipets. The experimental conditions used for both native and deglycosylated channel recordings were strictly identical; in particular, BTX (200 nM) was added in the pipet solution to produce steady-state activation of both kinds of channels. In addition, the bilayer-forming composition was a 5:4:1 PE/PS/PC mixture at a total lipid concentration of 1 mg/mL in hexane, as with the native channel, and the electrolyte solution was 0.5 M NaCl and 5 mM HEPES (pH 7.4) on both sides (in the pipet and in the external bath). Conductance experiments were performed at room temperature (~ 20 °C).

Modeling of the Sodium Channel. The crystal structure of the KcsA potassium channel [Protein Data Bank (PDB) entry 1BL8 (5)] was used as the template structure for homology modeling of the S5 and S6 transmembrane regions and the pore helices of the four sodium channel domains. ClustalW (18) and Modeller4 (19) were used for sequence alignment and model generation, respectively. Because the S5–S6 linker (P-loop) is much larger in the sodium channel than in the potassium channel structures, there were no directly comparable sequences for alignment of this region. Lipkind and Fozzard (20) proposed, on the basis of secondary structure predictions, probable evolutionary conservation with potassium channels, toxin binding modeling, and aromatic residue locations, that the regions of the P-loops which contain the selectivity filter residues formed an α -helix–turn– β -strand motif. This motif was built using the SYBYL modeling package (Tripos Inc., version 6.8). The Protein Data Bank (21) was searched using BLAST (22) for structures sharing sequence homology with the P-loop sections N-terminal to the α -helix–turn– β -strand structures. The sequence of one hit [PDB entry 1MQ8, chain B (23)] was $> 65\%$ similar with a 60-residue section of the domain I P-loop and a 30-residue section of the domain III P-loop; Modeller4 was used to create homology models of these sections. The remaining sections of the P-loops were built in SYBYL according to the consensus of a number of secondary structure prediction algorithms (24). The homology models and secondary structural elements were positioned with residues accessible according to available biochemical data, in particular, that described by Li et al. (25). Loops were added between the positioned structural elements using the “loop search” function in SYBYL and were assessed for consistency with biochemical data.

The five putative glycosylation sites were identified manually as conserved Asn-X-Ser or -Thr sequences in the P-loops (Figure 1), and confirmed using the NetNGlyc site (<http://www.cbs.dtu.dk/services/NetNGlyc>) which predicts N-glycosylation sites for human proteins using a neural network approach.

Coordinates for pentameric core carbohydrate moieties were obtained from the crystal structure of the influenza neuraminidase glycoprotein [PDB entry 1F8B (26)], and attached using SYBYL to Asn277, Asn287, and Asn316 of domain I and to Asn1159 and Asn1173 of domain III. The final model was subjected to 100 rounds of conjugate gradient minimization in SYBYL using the Tripos force field.

RESULTS

Purification of Native and Deglycosylated Sodium Channels. Sodium channels from electric eel electroplax membranes were purified as previously described either using affinity chromatography on an anti-*N*-acetylneuraminic acid antibody column (2) or using a lectin affinity column preceded by ion exchange and followed by gel filtration. Wheat germ lectin binds NAG and *N*-acetylneuraminic acids, whereas the IgM more specifically binds poly- α -2,8-*N*-neuraminic acids. Hence, there is slightly greater heterogeneity due to the sugars in the lectin-derived preparation, and consequently, the yield of purified protein from this method is considerably larger.

Purified proteins (Figure 2a) were subjected to deglycosylation by the PGNase F enzyme, which cleaves between the innermost NAG sugar and the asparagine residue of the polypeptide to which it is attached. The deglycosylated proteins ran on SDS gels with a lower apparent molecular mass (~ 210 kDa) than the native protein (~ 240 – 300 kDa), but consistent with the calculated mass of the protein component alone. The band of the deglycosylated preparation was much narrower (Figure 2a) because of the loss of heterogeneity arising from the sugar components. The deglycosylated samples produced from the two types of native preparations were indistinguishable on gels and spectroscopically (data not shown). On Western blots developed using the antibody against *N*-acetylneuraminic acid (Figure 2b), no sugars were detected in the deglycosylated sample; extensive staining was seen for the native protein.

Conductance Properties of Native and Deglycosylated Sodium Channels. To characterize the functional effects of deglycosylation, single-channel activity was recorded for deglycosylated sodium channels after reconstitution into planar lipid bilayers, and compared to native channel recordings previously obtained (2). Both types of preparations were assayed in the presence of BTX, which allowed monitoring of steady-state activation. Representative single-channel patterns of activity are shown for native (Figure 3a) and deglycosylated (Figure 3b) channels. Whereas the native channel yields only fairly well resolved closed–open transitions with a long duration with a single-channel conductance of 18 pS, the deglycosylated channel also appears to produce less well-resolved subconductance states. For example, a continuous recording shown in Figure 3b begins with a stepwise transition of 13 pS and is then followed by a rapid flickering which stabilizes to a lower (8.5 pS) subconductance state, followed by two other similar transitions. The

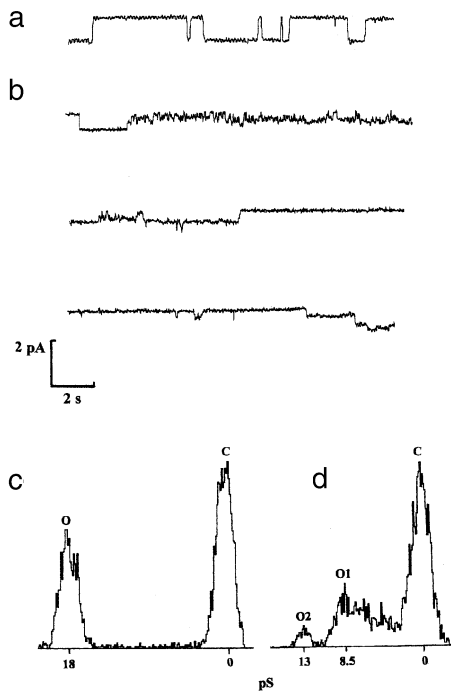


FIGURE 3: Comparison of single-channel activity displayed by (a) native and (b) deglycosylated purified and BTX-treated sodium channels in planar lipid bilayers at the tip of patch pipets. The scale bars apply to all traces, and the holding voltage was 60 mV throughout. Openings are downward deflections. Conductance amplitude histograms of (c) native and (d) deglycosylated channels are shown.

amplitude histograms (Figure 3c,d) highlight the rather different conductance distributions exhibited by the two preparations. In addition, the opening probability (at the same applied voltage) is reduced for the deglycosylated channel, as compared with that of the native channel, in agreement with the depolarizing shift of activation previously reported (14).

CD Spectroscopy of the Binding of Ligands to Deglycosylated Channels. CD spectroscopic studies were undertaken in a manner similar to that previously described (2) to ascertain whether the deglycosylated sodium channels respond in an analogous way to the native channel upon binding of BTX and LTG. As was found for native channels, there was an increase of $\sim 20\%$ in the peaks at 221 and 208 nm (data not shown), and a concomitant increase in the calculated helical content, suggesting that deglycosylated proteins are still able to undergo state-dependent changes induced by these ligands.

Structural Characterization of Deglycosylated Sodium Channels. SRCD spectroscopy was used to compare the secondary structures of the purified sodium channel protein in its native and its deglycosylated forms, because it allows collection of data to lower wavelengths than conventional CD, and hence enabled the examination of the effects of the sugar on the spectrum. These studies utilized channel proteins in lipid/detergent mixed micelles, where absorption and flattening effects that can be associated with membrane samples are negligible (27).

To examine whether the spectra of the missing sugars could simply account for the differences between the native and deglycosylated spectra, the following procedures were undertaken. (1) The native and deglycosylated channel

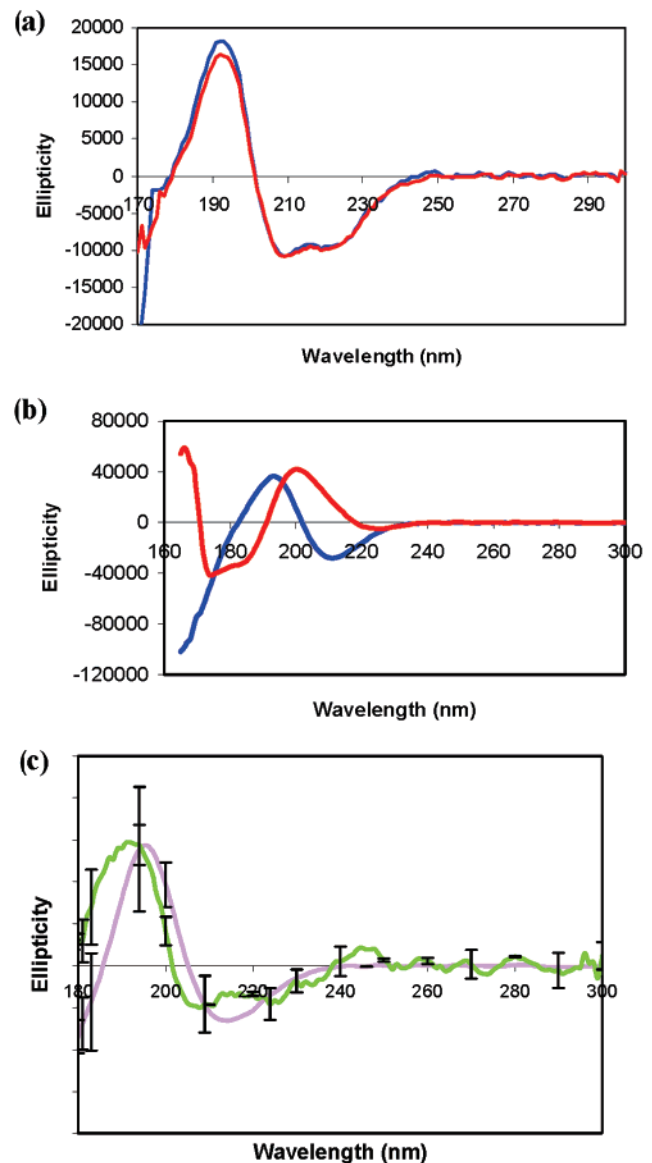


FIGURE 4: Synchrotron radiation circular dichroism spectra: (a) native (blue) and deglycosylated (red) channels, (b) colominic acid (red) and chitopentose (blue) sugars, and (c) difference spectra (native minus deglycosylated) of channels (green) and net equivalent sugar spectra (purple). Error bars (one standard deviation) in the measurements are shown.

spectra were measured at the same protein concentrations, so they could be compared directly (Figure 4a). To produce the “difference” spectrum (Figure 4c), the native spectrum was subtracted from the deglycosylated spectrum. (2) The spectra of colominic acid and chitopentose (Figure 4b) (which were both measured at the same concentrations in terms of milligrams per milliliter) were multiplied by 0.4 and 0.45, respectively, to reflect their relative (by mass) contributions to the native channel spectrum, and summed. Then, to put them on the same scale as the protein, as they were measured at an effective concentration 4 times greater than that of the protein (20 mg/mL in a 0.001 cm cell vs 1 mg/mL in a 0.005 cm cell for the protein), the net sugar spectrum was multiplied by 0.25. Finally, as the sugars contribute approximately 30% of the total mass, the net spectrum was multiplied by a factor of 0.3/0.7, which should produce a spectrum (Figure 4c) with the same magnitude as their contribution in the native glycoprotein spectrum (this

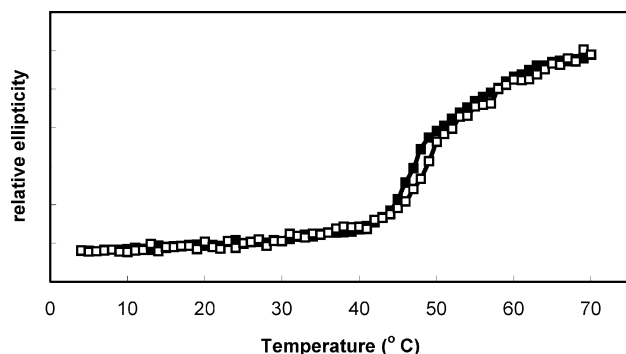


FIGURE 5: Circular dichroism thermal denaturation curves of native (\square) and deglycosylated (\blacksquare) sodium channels. The ellipticities were monitored at a wavelength of 223 nm over the temperature range from 4 to 70 °C.

is designated the “equivalent sugar spectrum”). Then, the equivalent sugar spectrum was plotted with the difference spectrum, and the two were compared (Figure 4c). Within the error limits of the measurements, the equivalent sugar spectrum and the difference spectrum were indistinguishable, suggesting that the spectral differences between native and deglycosylated channels can be entirely attributed to the missing sugars.

Thermal Denaturation of Native and Deglycosylated Channels. The native channels and the deglycosylated channels were monitored for thermal stability at 223 nm, a wavelength at which the sugars do not produce a CD signal, but which is sensitive to protein conformational changes, especially those involving helical content. Both native and deglycosylated proteins produced sigmoidal curves with T_m values of approximately 48–50 °C, the inflection point being at a slightly higher value for the native form (Figure 5). This result suggests that both samples undergo cooperative unfolding, that both forms are quite stable in a micellar environment, and that the deglycosylated channel is not significantly less stable than the native form.

Modeling of Sugar Binding Sites on the Sodium Channel. A total of five glycosylation sites are predicted to be on Asn residues in the domain I and domain III S5–S6 extracellular loops of the eel protein (Figure 1). Similar putative glycosylation sites are found at comparable positions in other sodium channels.

The homology model of the sodium channel based on the KcsA crystal structure (5) is shown in Figure 6. It was built to provide a general schematic model of where the sugars will be located with respect to the channel lumen. Good structural homologues do not exist for the extracellular loops, which therefore were constructed with reference to secondary structure predictions and relevant biochemical data, as a means of providing an anchor site for the carbohydrates. However, additional data are most certainly required for more accurate modeling before this pharmacologically important region of the channel can be interpreted in terms of its role in toxin binding, selectivity filter, and slow inactivation.

The pentose carbohydrate moieties used in the model [Man(α 1–3)Man(α 1–6)Man(β 1–4)NAG(β 1–4)NAG] contain the trimannosyl cores attached to two inner NAGs that are typically found in N-glycosylated proteins. The full sugar chains were not modeled because of the current uncertainty of their exact composition and the lack of good structural models for extended sugar chains. Obviously, the native

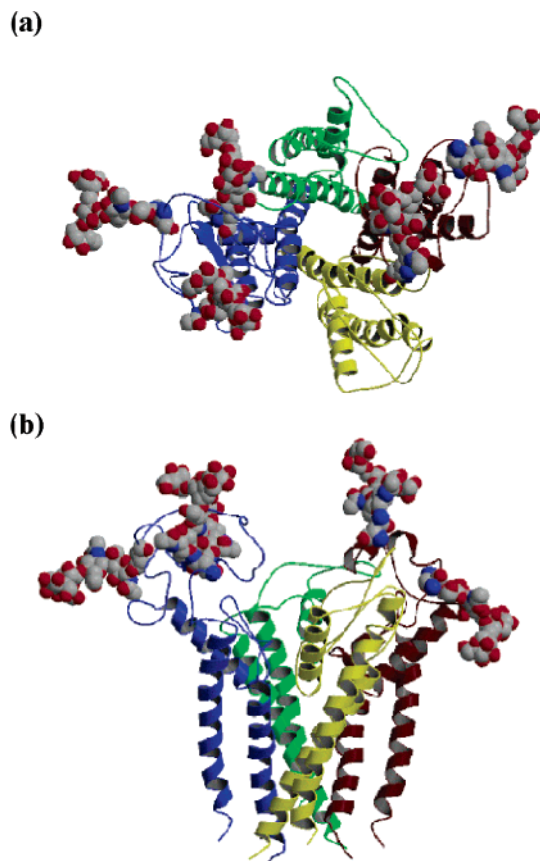


FIGURE 6: Molecular model for the sodium channel highlighting potential N-glycosylation sites: (a) top view and (b) side view. Each of the four domains of the protein is displayed in a different color in ribbon format. The core sugars and their attached Asn residues at each putative glycosylation site are depicted in space-filling format. This figure was created using MOLSCRIPT (40) and Raster3D (41).

sugar chains extend to significantly greater lengths than shown in this model. Nevertheless, the short sugars serve the purpose of providing a model for visualizing the general localization of the sugar attachments on the extracellular surface of the channel. Clearly, the negatively charged sugar moieties present in the sodium channel will impinge on the extracellular vestibule of the channel, and it is reasonable to expect that their large negative charge will considerably influence the electrostatics at the channel entrance.

DISCUSSION

Influence of Deglycosylation on Channel Properties and Effects of LTG. It was previously hypothesized (14, 28, 29) that sialic acids may influence the local electric fields near sodium channels, especially at the entrance to the pore, since the sugars are attached to sites in the P-loops between the S5 and S6 helices. Consequently, deglycosylation should decrease the large number of negative charges, and likely diminish the sodium ion density in the external pore antechamber. These two effects (altered transmembrane electric field experienced by voltage sensors and decreased sodium ion density) could contribute to the observed electrophysiological modifications: voltage shifts of macroscopic conductance parameters (especially steady-state inactivation and activation) and a slightly reduced single-channel conductance and/or substates (14, 28, 29).

In earlier work, some variability was observed for the electrophysiological effects of sodium channels after partial deglycosylation (14). Overall, however, after neuraminidase treatment, there tended to be a slightly reduced single-channel conductance and decreased probability of the main open state with a much broader distribution and subconductance states. In our preparations using a different enzyme to achieve a more complete deglycosylation, small but significant differences in single-channel conductances of native and deglycosylated sodium channels were found. The average unit conductance was reduced by ~ 5 pS (i.e., nearly 30%) for the deglycosylated channels with respect to the native channels, and there was evidence for smaller subconductance states.

Another measure of a functional property of sodium channels is the state-dependent change detected by CD spectroscopy (2). Similar spectral changes in the presence of LTG and BTX were found for native and deglycosylated channels, suggesting the deglycosylated channels also retain this type of activity.

Biological Implications of Deglycosylation. Deglycosylation is generally believed to be associated with modified function through either a hyperpolarizing shift of steady-state inactivation or a depolarizing shift of steady-state activation. These electrophysiological manifestations at the macroscopic sodium current level translate to a smaller "activation window".

The role of glycosylation in voltage-dependent channel gating for the cloned human cardiac sodium channel and the adult rat skeletal muscle isoform has been investigated in HEK293 cells transiently transfected with the corresponding cDNA (30). Pretreatment of transfected cells with neuraminidase resulted in significant (4–12 mV) shifts in the steady-state activation of opposite directions according to the channel isoform considered (depolarizing shift with the human cardiac sodium channels and hyperpolarizing shift with the skeletal muscle sodium channels). On the other hand, there were no significant effects on single-channel conductance, the mean open time, or the open probability (30).

Glycosylation is developmentally regulated and is directly correlated with channel functional modifications. For example, the developmental change in the glycosylation state of Na(v)1.9, a TTX-resistant isoform of the voltage-gated sodium channel, in native dorsal root ganglion is paralleled by shifts of steady-state inactivation (31). Whole-cell patch-clamp analysis demonstrated that the midpoint of steady-state inactivation is shifted 7 mV in a hyperpolarized direction in neonatal compared with adult dorsal root ganglion neurons, although there is no significant difference in activation. This resulted in a smaller activation window and reduced firing. In agreement with this, it was also recently found that deficient glycosylation of cardiac sodium channels (also TTX-resistant) contributed to arrhythmogenesis in heart failure (32). In other systems, the sodium channel $\beta 1$ subunits (absent in the electroplax) have been shown to be heavily glycosylated, and these have substantial effects on gating (33).

Effects of Deglycosylation on the Channel Structure. Since approximately 30% of the sodium channel glycopeptide mass is carbohydrate, mostly *N*-acetylhexosamines and sialic acids (11), it was expected that the CD spectrum, and consequently the protein secondary structure, of the deglycosylated chan-

nels could well differ from those of native channels, either due to a change in protein conformation or due to the removal of a sugar signal. Hence, the simple spectral consequences arising from the presence of sugars needed to be considered first.

Normally, sugars give rise to significant CD spectra only at wavelengths below 180 nm. Hence in this study, SRCD was used so that data could also be collected in the VUV region, where the sugars absorb. Sugars rarely produce significant dichroic signals in the UV region between 190 and 240 nm, so their contributions to glycoprotein UV CD spectra are generally ignored. However, both sialic acid and NAG do have measurable spectral transitions in this wavelength range (34, 35), which had to be considered in the difference analyses with native and deglycosylated proteins. The sugars on sodium channels are complex, unknown structures, but their composition is known to be oligomers of *N*-acetylneuraminic acid and NAG. To mimic their spectra, we used polymeric *N*-acetylneuraminic acid in the form of colominic acid, and an oligosugar of NAG, in the form of chitopentose. These were used instead of the monomeric sugars, as there is reported to be a moderate chain length dependence of the spectrum of these sugars (34), which would result in larger signals per monomer for oligomers than for monomers, although the incremental increase tails off significantly as the sugars increase in length. Because the sugars used as models in this study are shorter than the actual sugars on the sodium channel, the contributions of sugars to the native channel spectra may be slightly larger than the contribution to the equivalent sugar spectrum calculated in this study. Furthermore, only the *N*-acetylneuraminic acid and NAG contributions are mimicked here. However, the 15% of the sugars that are not *N*-acetylneuraminic acid or NAG are not amino sugars (they are mostly mannose and galactose), and so are unlikely to make significant contributions to the channel spectra in this wavelength range.

Although the spectra of the isolated chitopentose and colominic acid sugars are substantial in magnitude (Figure 4b), they nearly mirror each other in sign, colominic acid having a positive peak at ~ 210 nm and a negative peak at ~ 190 nm and chitopentose having a negative peak at ~ 215 nm and a positive peak ~ 190 nm. Hence, their net spectrum (Figure 4c) is close to zero with only a small positive peak around 200 nm.

The magnitude of the difference spectrum between native and deglycosylated channels also is quite small (peak maximum at ~ 200 nm, and rather featureless at other wavelengths). When the difference spectrum is plotted with the equivalent sugar spectrum (Figure 4c), the two are indistinguishable at a significance level above the error levels in the measurements. Hence, it appears that the sugar contribution alone can account for the net differences between the native and deglycosylated proteins. Of course, it is always possible that exactly compensating secondary structural changes in different parts of the molecule could produce net spectra that are identical, which would not be detected by this method, but this is considered unlikely.

The thermal denaturation studies indicate that the tertiary conformations and stabilities of the deglycosylated form and the native form do not differ significantly. This, together with the likelihood that sugar signals can entirely account for the

observed differences in the SRCD spectra, suggests that conformational effects are not the reason for the observed alterations in the voltage dependence of channel activation and inactivation observed on desialylation, and are consistent with the electrostatic hypothesis for the influence of the sialic acids on the transmembrane potential (14, 28, 29).

Molecular Modeling of Sugar Sites at the Channel Vestibule. A molecular model for the sodium channel, including the putative sites for sugar binding, was constructed. It provided visual evidence that the sugars at the channel periphery adjacent to the vestibule are in positions which could have a significant effect on the electrostatics of the channel, influencing the channel function, but not necessarily modifying the channel polypeptide structure.

Comparisons with Deglycosylation Studies on Other Channels and Consequences for Future Structural Studies. The structural and functional results found for sodium channels in this study are in direct contrast to the results in a similar study on aquaporins, which found there was a small conformational change in the protein after deglycosylation (36) while the single-channel water permeability was virtually unchanged. In that case, there was a structural but not a functional alteration, whereas in our case, there was a functional but no structural alteration.

The oligosaccharides in the voltage-gated sodium channels produce considerable heterogeneity in the protein, as seen by the broad bands they form on SDS-PAGE gels. This heterogeneity, in addition to the flexibility of the long sugars, would tend to be detrimental to attempts to crystallize the protein. This preparation, which eliminates both of these problems, would then seem to be more appropriate as a starting point for crystallization trials. Interestingly, the only ion channels for which high-resolution crystal structures currently exist are potassium channels from bacterial sources (5, 37, 38), which have no naturally occurring sugars to interfere with the process. Additionally, deglycosylation of aquaporin was found to be important for producing higher-resolution two-dimensional crystals for cryo-electron microscopy (39). Therefore, the deglycosylated protein prepared in this study may be more suitable for structural studies.

In summary, deglycosylated sodium channels were shown to be functionally similar as far as steady-state activation is concerned, but with a single-channel conductance level slightly lower than that of native channels. CD studies showed that the deglycosylated channels maintained the Lamotrigine- and batrachotoxin-induced structural changes associated with channel functional states previously observed for native channels. SRCD studies showed that following deglycosylation, the net secondary structures and thermal stability profiles of the channels are unchanged. Thus, the effects of deglycosylation appear to result from electrostatic effects due to the loss of the large negative charge from the sugars at the mouth of the channel, rather than a conformational change in the protein.

ACKNOWLEDGMENT

We thank Dr. Robert W. Janes of Queen Mary College, University of London, for Lamotrigine, Dr. R. Schneerson of the National Institutes of Health for the horse antiserum, and Dr. J. W. Daly of the National Institutes of Health for batrachotoxin. H.D. acknowledges the help of Glenn Alder

in some of the conductance experiments carried out in St. George's Hospital Medical School (London, U.K.) and Dr. C. L. Bashford for his hospitality. We thank Dr. Robert W. Janes (Queen Mary College), Dr. Frank Wien, A. Miles, and J. G. Lees (all from Birkbeck College) for help with the SRCD experiments.

REFERENCES

1. Yu, F. H., and Catterall, W. A. (2003) Overview of the voltage-gated sodium channel family, *Genome Biol.* 4, 207–209.
2. Cronin, N. B., O'Reilly, A., Ducholier, H., and Wallace, B. A. (2003) Binding of the anticonvulsant drug lamotrigine and the neurotoxin batrachotoxin to voltage-gated sodium channels induces conformational changes associated with block and steady-state activation, *J. Biol. Chem.* 278, 10675–10682.
3. Noda, M., Shimizu, S., Tanabe, T., Takai, T., Kayano, T., Ikeda, T., Takahashi, H., Nakayama, H., Kanaoka, Y., Minamino, N., Kangawa, K., Matsuo, H., Raftery, M. A., Hirose, T., Inayama, S., Hayashida, H., Miyata, T., and Numa, S. (1984) Primary structure of *Electrophorus electricus* sodium channel deduced from cDNA sequence, *Nature* 312, 121–127.
4. Durell, S. R., Hao, Y., and Guy, H. R. (1998) Structural models of the transmembrane region of voltage-gated and other K⁺ channels in open, closed, and inactivated conformations, *J. Struct. Biol.* 121, 263–284.
5. Doyle, D. A., Cabral, J. M., Pfuetzner, R. A., Kuo, A., Gulbis, J. M., Cohen, S. L., Chait, B. T., and MacKinnon, R. (1998) The structure of the potassium channel: Molecular basis of K⁺ conduction and selectivity, *Science* 280, 69–77.
6. Plummer, N. W., and Meisler, M. (1999) Evolution and diversity of mammalian sodium channel genes, *Genomics* 57, 323–331.
7. Goldin, A. L., Barchi, R. L., Caldwell, J. H., Hofmann, F., Howe, J. R., Kallen, R. G., Mandel, G., Meisler, M. H., Netter, Y. B., Noda, M., Tamkun, M. M., Waxman, S. G., Wood, J. N., and Catterall, W. A. (2000) Nomenclature of voltage-gated sodium channels, *Neuron* 28, 365–368.
8. Goldin, A. L. (2001) Resurgence of sodium channel research, *Annu. Rev. Physiol.* 63, 871–894.
9. Hanlon, M. R., and Wallace, B. A. (2002) Structure and function of voltage-dependent ion channel regulatory β subunits, *Biochemistry* 41, 2886–2894.
10. Bennett, E. S. (2002) Isoform-specific effects of sialic acid on voltage-dependent Na⁺ channel gating: Functional sialic acids are localized to the S5–S6 loop of domain I, *J. Physiol.* 538, 675–690.
11. Agnew, W. S., Cooper, E. C., James, W. M., Tomiko, S. A., Rosenberg, R. L., Emerick, M. C., Correa, A. M., and Zhou, J. Y. (1988) In *Molecular Biology of Ion Channels* (Agnew, W. S., Claudio, T., and Sigworth, F. J., Eds.) pp 329–365, Academic Press, San Diego.
12. James, W. M., and Agnew, W. S. (1987) Multiple oligosaccharide chains in the voltage-sensitive Na channel from *Electrophorus electricus*: Evidence for α -2,8-linked polysialic acid, *Biochem. Biophys. Res. Commun.* 148, 817–826.
13. Yabe, U., Sato, C., Matsuda, T., and Kitajima, K. (2003) Polysialic acid in human milk. CD36 is a new member of mammalian polysialic acid-containing glycoprotein, *J. Biol. Chem.* 278, 13875–13880.
14. Bennett, E., Urcan, M. S., Tinkle, S. S., Koszowski, A. G., and Levinson, S. R. (1997) Contribution of sialic acid to the voltage dependence of sodium channel gating. A possible electrostatic mechanism, *J. Gen. Physiol.* 109, 327–343.
15. Allen, P. Z., Glode, M., Schneerson, R., and Robbins, J. B. (1982) Identification of immunoglobulin heavy-chain isotypes of specific antibodies of horse 46 group B meningococcal antiserum, *J. Clin. Microbiol.* 15, 324–329.
16. James, W. M., Emerick, M. C., and Agnew, W. S. (1989) Affinity purification of the voltage-sensitive sodium channel from electropex with resins selective for sialic acid, *Biochemistry* 28, 6001–6009.
17. Hanke, W., Methfessel, C., Wilmsen, G., and Boheim, G. (1984) Ion channel reconstitution into planar lipid bilayers on glass pipettes, *Bioelectrochem. Bioenerg.* 12, 329–339.
18. Thompson, J. D., Higgins, D. G., and Gibson, T. J. (1994) CLUSTAL W: Improving the sensitivity of progressive multiple

- sequence alignment through sequence weighting, position-specific gap penalties and weight matrix choice, *Nucleic Acids Res.* 22, 4673–4680.
19. Sali, A., and Blundell, T. L. (1993) Comparative protein modelling by satisfaction of spatial restraints, *J. Mol. Biol.* 234, 779–815.
 20. Lipkind, G. M., and Fozzard, H. A. (2000) KcsA crystal structure as framework for a molecular model of the Na⁺ channel pore, *Biochemistry* 39, 8161–8170.
 21. Berman, H. M., Westbrook, J., Feng, Z., Gilliland, G., Bhat, T. N., Weissig, H., Shindyalov, I. N., and Bourne, P. E. (2000) The Protein Data Bank, *Nucleic Acids Res.* 28, 235–242.
 22. Altschul, S. F., Gish, W., Miller, W., Myers, E. W., and Lipman, D. J. (1990) Basic local alignment search tool, *J. Mol. Biol.* 215, 403–410.
 23. Shimaoka, M., Xiao, T., Liu, J. H., Yang, Y., Dong, Y., Jun, C. D., McCormack, A., Zhang, R., Joachimiak, A., Takagi, J., Wang, J. H., and Springer, T. A. (2003) Structures of the α L I domain and its complex with ICAM-1 reveal a shape-shifting pathway for integrin regulation, *Cell* 112, 99–111.
 24. Combet, C., Blanchet, C., Geourjon, C., and Deléage, G. (2000) NPS@: Network protein sequence analysis, *Trends Biochem. Sci.* 25, 147–150.
 25. Li, R., Vélez, P., Chiamvimonvat, N., Tomaselli, G., and Marbán, E. (2000) Charged residues between the selectivity filter and S6 segments contribute to the permeation phenotype of the sodium channel, *J. Gen. Physiol.* 115, 81–92.
 26. Smith, B. J., Colman, P. M., Von Itzstein, M., Danylec, B., and Vargese, J. N. (2001) Analysis of inhibitor binding in influenza virus neuraminidase, *Protein Sci.* 10, 689–696.
 27. Wallace, B. A., and Mao, D. (1984) Circular dichroism analyses of membrane proteins: An examination of light scattering and absorption flattening in large membrane vesicles and membrane sheets, *Anal. Biochem.* 142, 317–328.
 28. Levinson, S. R., Thornhill, W. B., Duch, D. S., Recio-Pinto, E., and Urban, B. W. (1990) The role of nonprotein domains in the function and synthesis of voltage-gated sodium channels, in *Ion Channels* (Narahashi, T., Ed.) Vol. 2, pp 33–64, Plenum Press, New York.
 29. Recio-Pinto, E., Thornhill, W. B., Duch, D. S., Levinson, S. R., and Urban, B. W. (1990) Neuraminidase treatment modifies the function of electroplax sodium channels in planar lipid bilayers, *Neuron* 5, 675–684.
 30. Zhang, Y., Hartmann, H. A., and Satin, J. (1999) Glycosylation influences voltage-dependent gating of cardiac and skeletal muscle sodium channels, *J. Membr. Biol.* 171, 195–207.
 31. Tyrrell, L., Renganathan, M., Dib-Hajj, S. D., and Waxman, S. G. (2001) Glycosylation alters steady-state inactivation of sodium channel Nav1.9/NaN in dorsal root ganglion neurons and is developmentally regulated, *J. Neurosci.* 21, 9629–9637.
 32. Ufret-Vincenty, C. A., Baro, D. J., Lederer, W. J., Rockman, H. A., Quinones, L. E., and Santana, L. F. (2001) Role of sodium channel deglycosylation in the genesis of cardiac arrhythmias in heart failure, *J. Biol. Chem.* 276, 28197–28203.
 33. Whisenand, T. D., Maue, R. A., Shah, R. M., and Levinson, S. R. (2001) The effect of B1 sialylation on sodium channel gating, *Biophys. J.* 80, 232a.
 34. Dickinson, H. R., and Bush, C. A. (1975) Circular dichroism of oligosaccharides containing neuraminic acid, *Biochemistry* 14, 2299–2304.
 35. Bystricky, S., Pavliak, V., and Szu, S. C. (1997) Characterization of colominic acid by circular dichroism and viscosity analysis, *Biophys. Chem.* 63, 147–152.
 36. van Hoek, A. N., Wiener, M. C., Verbavatz, J. M., Brown, D., Lipniunas, P. H., Townsend, R. R., and Verkman, A. S. (1995) Purification and structure–function analysis of native, PNGase F-treated, and endo- β -galactosidase-treated CHIP28 water channels, *Biochemistry* 34, 2212–2219.
 37. Jiang, Y. X., Lee, A., Chen, J. Y., Cadene, M., Chait, B. T., and MacKinnon, R. (2002) Crystal structure and mechanism of a calcium-gated potassium channel, *Nature* 417, 515–522.
 38. Kuo, A., Gulbis, J. M., Antcliff, J. F., Rahman, T., Lowe, E. D., Zimmer, J., Cuthbertson, J., Ashcroft, F. M., Ezaki, T., and Doyle, D. A. (2003) Crystal structure of the potassium channel KirBac1.1 in the closed state, *Science* 300, 1922–1926.
 39. Cheng, A., van Hoek, A. N., Yeager, M., Verkman, A. S., and Mitra, A. K. (1997) Three-dimensional organization of a human water channel, *Nature* 387, 627–630.
 40. Kraulis, P. J. (1991) MOLSCRIPT: A program to produce both detailed and schematic plots of protein structures, *J. Appl. Crystallogr.* 24, 946–950.
 41. Merritt, E. A., and Bacon, D. J. (1997) Raster3D: Photorealistic molecular graphics, *Methods Enzymol.* 277, 505–524.

BI048741Q